

Molecular dynamics study of thermal expansion and compression in spin-crossover solids using a microscopic model of elastic interactions

Masamichi Nishino,^{1,2,5,*} Kamel Boukheddaden,³ and Seiji Miyashita^{4,5}

¹Computational Materials Science Center, National Institute for Materials Science, Tsukuba, Ibaraki 305-0047, Japan

²Department of Theoretical and Computational Molecular Science, Institute for Molecular Science, Okazaki, Japan

³Groupe d'Etudes de la Matière Condensée, CNRS-Université de Versailles-St. Quentin en Yvelines, 45 Avenue des Etats Unis, F78035 Versailles Cedex, France

⁴Department of Physics, Graduate School of Science, The University of Tokyo, Bunkyo-Ku, Tokyo, Japan

⁵CREST, JST, 4-1-8 Honcho Kawaguchi, Saitama 332-0012, Japan

(Received 17 November 2008; published 28 January 2009)

We study characteristic features of the temperature and pressure dependences of the volume and high-spin fraction of spin-crossover solids. We develop a model and method of molecular dynamics (MD) in the isobaric-isothermal ensemble to treat the motion of the intramolecular totally symmetric mode, taking into account the entropy effect from other modes. We find several interesting observations, e.g., a nonmonotonic temperature dependence of the volume. Sigmoidal relaxations from the excited high-spin state (photoinduced state), which were often observed in experiments, are automatically reproduced in the present deterministic dynamics of MD, although it has previously been studied by assuming Arrhenius transition probabilities in stochastic dynamics.

DOI: 10.1103/PhysRevB.79.012409

PACS number(s): 75.30.Wx, 64.60.-i, 75.50.Xx, 75.60.-d

Spin-crossover (SC) complexes have attracted much attention for their potential applicability to electronic devices, e.g., optical data storage, optical sensors, etc. They exhibit switching phenomena between the low-spin (LS) and high-spin (HS) states, i.e., SC transitions by change of external perturbations such as temperature, pressure, magnetic field, light irradiation, etc.¹⁻⁷ It is considered that the cooperative nature of the interactions between molecules is the key to understand the mechanisms of SC transitions.

For studies of the cooperative nature, Ising-like models have often been studied because of their simple descriptions.⁸⁻¹² On the other hand, several studies have been done on the role of elastic interactions, and their importance in SC has been pointed out.¹³⁻²⁴

It is well admitted that entropy effects are a key factor for SC phenomena. The entropy change between the LS and HS states, $\Delta S = Nk_B \ln \frac{g_{\text{HS}}}{g_{\text{LS}}}$, takes place with $\frac{g_{\text{HS}}}{g_{\text{LS}}} = O(100) - O(1000)$ in experiments, where N is the number of molecules and $\frac{g_{\text{HS}}}{g_{\text{LS}}}$ is the ratio of degeneracies between the HS and LS states. The dominant contribution to the entropy is intramolecular vibrations with many modes.²⁵

In a previous study,²¹ we attributed the entropy difference between the LS and HS states to one intramolecular vibrational mode (totally symmetric mode), where different frequencies of the HS and LS states ($\frac{g_{\text{HS}}}{g_{\text{LS}}} = \frac{1/\omega_{\text{HS}}}{1/\omega_{\text{LS}}} = 10$) were given. Thus, the potential there was unrealistically deformed (in real compounds, $\frac{1/\omega_{\text{HS}}}{1/\omega_{\text{LS}}} \simeq 2$). Although we succeeded to capture characteristic features of the SC transition, the value $\frac{g_{\text{HS}}}{g_{\text{LS}}} = 10$ was still small compared with realistic values $O(100) - O(1000)$. Even for this value, we sacrificed the realistic potential form. Therefore, investigations of detailed features and quantitative analyses of SC phenomena were impossible. In general, in MD, the density of state, i.e., the entropy is determined by a given potential uniquely and it is difficult to control it arbitrarily.

In order to investigate quantitatively the dependences of the system volume and the HS fraction on external perturbations, e.g., temperature, pressure, etc. and also dynamical properties, it is necessary to have a formulation to use a realistic intramolecular potential for the totally symmetric mode and simultaneously to treat a large $\frac{g_{\text{HS}}}{g_{\text{LS}}}$ mainly originating from other modes and spins. In the present study, we develop a model and method which enables us to realize this goal. We also extend the model to control not only temperature (T) but also pressure (P). We give equations of real-time dynamics of molecular dynamics (MD) for the isobaric-isothermal (i.e., N, P, T) ensemble.

Applying this unique formulation, we find nontrivial behavior of the T dependences of the system volume (V) and the HS fraction (f_{HS}) under constant pressure. We also investigate relaxation dynamics from the excited HS state (photoinduced state) for various T and P . In experiments, characteristic sigmoidal curves in the relaxation process were often observed,²⁶ and Arrhenius transition probabilities¹⁰ have been assumed to reproduce them in Monte Carlo methods. Here, we obtain sigmoidal curves automatically in the present MD simulations.

First, we consider the following Hamiltonian:²¹

$$\mathcal{H}_0 = \sum_{i=1}^N \frac{\mathbf{p}_i^2}{2M} + \sum_{i=1}^N \frac{p_i^2}{2m} + \sum_{i=1}^N V_i^{\text{intra}}(r_i) + \sum_{\langle i,j \rangle} V_{ij}^{\text{inter}}(\mathbf{X}_i, \mathbf{X}_j, r_i, r_j). \quad (1)$$

The intramolecular potential energy $V_i^{\text{intra}}(r_i)$ is a function of the radius r_i of the i th molecule, p_i is the corresponding momentum, and m is the mass. Here, $\{r_i, p_i\}$ represents the motion of the totally symmetric mode, which is the most important mode.²⁵ The intermolecular potential between the i th and j th molecules is denoted by $V_{ij}^{\text{inter}}(\mathbf{X}_i, \mathbf{X}_j, r_i, r_j)$, where $\mathbf{X}_i = (X_i, Y_i)$ is the coordinate of the center of the i th molecule

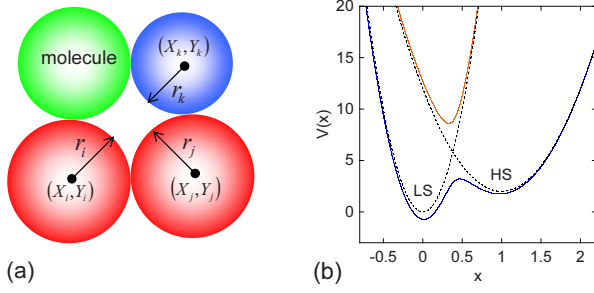


FIG. 1. (Color online) (a) Molecules of LS (blue, upper right), HS (red, lower), and intermediate (green, upper left) states. (b) Intramolecular potentials $V(x)_-$ (blue, lower) for the ground state and $V(x)_+$ (red, upper) for the excited state. x is the growth of r from r_{LS} . The broken lines are LS (left) and HS (right) potentials.

[see Fig. 1(a)]. The corresponding momentum is $\mathbf{P}_i = (P_{X_i}, P_{Y_i})$, and the mass of the molecule is M .

The intramolecular LS potential ($y=ax^2$) and HS one [$y=b(x-c)^2+d$] [see Fig. 1(b), broken lines] are mixed by the off-diagonal element J , which causes the intramolecular adiabatic potentials^{20,21,24} for the symmetric mode: $V(x)_\pm = \frac{A}{2} \{d+b(c-x)^2+ax^2 \pm \sqrt{4J^2+[d+b(c-x)^2-ax^2]^2}\}$. The functions $V(x)_\pm$ are plotted in Fig. 1(b), where x is defined as the difference of the radius from that of the ideal LS state (r_{LS}): $r=r_{LS}+x$. We adopt the double-well potential $V(x)_-$ for $V_i^{\text{intra}}(r_i)$, where $x=0$ and 1 correspond to ideal LS and HS states, respectively. The radius of the ideal HS state is thus $r_{HS}=r_{LS}+1$.

The entropy difference due to the intramolecular potential between the LS and HS states is given by $\Delta S=S_{HS}-S_{LS}=Nk_B \ln \frac{\omega_{LS}}{\omega_{HS}}$, where $\omega_{LS}=\sqrt{2a/m}$ and $\omega_{HS}=\sqrt{2b/m}$. In the present study, a realistic value of the ratio, $\frac{\omega_{LS}}{\omega_{HS}}=2$, is adopted.²⁵ For this purpose, we take $a=4$ and $b=1$, and we set the other parameters for $V_i^{\text{intra}}(r_i)$ as $A=10$, $c=1.0$, $d=0.2$, $J=0.3$, and $r_{LS}=9$.

Since \mathcal{H}_0 provides a small entropy change $\Delta S \approx Nk_B \ln 2$, it needs to include the entropy difference from other degrees of freedom, i.e., other intramolecular vibrations and also spins. We express the potential of other intramolecular vibrations as $V'=\sum_k m_k \omega_k^2 u_k^2/2$, where k is the index of modes. The value of ω_k may differ in the LS (ω_k^{LS}) and HS (ω_k^{HS}) states.⁹ The ratio of the total densities of states of these modes for the LS and HS states is described as $\prod_k \frac{\omega_k^{\text{LS}}}{\omega_k^{\text{HS}}}$ for each molecule.⁹ The degeneracy of spin ($2\hat{S}+1$) also contributes to the extra entropy. Thus, the entropy change due to these modes and spins is given by $\Delta S' \approx Nk_B \ln \prod_k \frac{\omega_k^{\text{LS}}}{\omega_k^{\text{HS}}} \frac{2\hat{S}^{\text{HS}}+1}{2\hat{S}^{\text{LS}}+1}$.

In order to express this extra entropy difference, we introduce an oscillator (u_{0i}) for each molecule,

$$\mathcal{H}_{\text{ph}} = \sum_{i=1}^N \frac{p_{0i}^2}{2m_0} + \sum_{i=1}^N \frac{1}{2} m_0 \bar{\omega}_{0i}^2 u_{0i}^2. \quad (2)$$

The eigenfunction (ground state) for $V(x)_-$ is $|\Psi_g(x)\rangle = \alpha(x)|\text{LS}(x)\rangle + \beta(x)|\text{HS}(x)\rangle$, and that for $V(x)_+$ is

$$|\Psi_e(x)\rangle = -\beta(x)|\text{LS}(x)\rangle + \alpha(x)|\text{HS}(x)\rangle.$$

Then,

$$\beta(x)^2 = |\langle \text{HS}(x) | \Psi_g(x) \rangle|^2$$

gives the HS component of each molecule.

The inverse of the frequency is proportional to the density of states of the oscillator, and thus $\bar{\omega}_{0i}$ is given by

$$\frac{1}{\bar{\omega}_{0i}} = \frac{\alpha(x_i)^2}{\bar{\omega}_{0LS}} + \frac{\beta(x_i)^2}{\bar{\omega}_{0HS}}, \quad (3)$$

where $\bar{\omega}_{0LS}$ and $\bar{\omega}_{0HS}$ are frequencies for the LS and HS states, and the ratio is given by $\frac{\bar{\omega}_{0LS}}{\bar{\omega}_{0HS}} = \prod_k \frac{\omega_k^{\text{LS}}}{\omega_k^{\text{HS}}} \frac{2\hat{S}^{\text{HS}}+1}{2\hat{S}^{\text{LS}}+1}$. In the present study, we set $\frac{\bar{\omega}_{0LS}}{\bar{\omega}_{0HS}}=100$ ($\bar{\omega}_{0HS}=1$). Because $\frac{\omega_{LS}}{\omega_{HS}}=2$, the ratio of the total densities of states is $\frac{g_{HS}}{g_{LS}}=200$.

Following Ref. 21, we adopt the intermolecular potential $V_{ij}^{\text{inter}}(\mathbf{X}_i, \mathbf{X}_j, r_i, r_j)$ between the nearest neighbors (i th and j th molecules) and next-nearest neighbors [i and k , see Fig. 1(a)], where D is the strength of the intermolecular interaction.

To control both pressure (P) and temperature (T) in this MD, the Andersen formalism with the Nosé-Hoover method²⁷⁻²⁹ is applied to this system. The Hamiltonian of the thermal reservoir and that for the pressure control are given by $\mathcal{H}_{\text{therm}} = \frac{p_s^2}{2Q} + 4Nk_B T \ln s$ and $\mathcal{H}_P = \frac{\Pi^2}{2M_{\Pi}} + PV$, respectively, where s is a scaling factor, P_s and Π are the conjugate momenta of s and the volume V , and Q and M_{Π} are effective masses associated with s and V , respectively.²⁷⁻²⁹ The total Hamiltonian including the external environment is given by $\mathcal{H}_{\text{total}} = \mathcal{H}_0 + \mathcal{H}_{\text{ph}} + \mathcal{H}_{\text{therm}} + \mathcal{H}_P$. Finally we have the following equations of motion for the real-time dynamics:

$$\frac{dr_i}{dt} = \frac{p_i}{m} + \frac{r_i}{n_d V} \frac{dV}{dt}, \quad (4)$$

$$\frac{dp_i}{dt} = -\frac{\partial V^{\text{intra}}}{\partial r_i} - \frac{\partial V^{\text{inter}}}{\partial r_i} - \frac{\partial V^{\text{ph}}}{\partial r_i} - \frac{p_i}{n_d V} \frac{dV}{dt} - \xi p_i, \quad (5)$$

$$\frac{dX_i}{dt} = \frac{P_i}{M} + \frac{X_i}{n_d V} \frac{dV}{dt}, \quad (6)$$

$$\frac{dP_i}{dt} = -\frac{\partial V^{\text{inter}}}{\partial X_i} - \frac{P_i}{n_d V} \frac{dV}{dt} - \xi P_i, \quad (7)$$

$$\frac{du_{0i}}{dt} = \frac{p_{0i}}{m_0}, \quad (8)$$

$$\frac{dp_{0i}}{dt} = -\frac{\partial V^{\text{ph}}}{\partial u_{0i}} - \xi p_{0i}, \quad (9)$$

$$\frac{ds}{dt} = s\xi, \quad (10)$$

$$\frac{d\xi}{dt} = \frac{1}{Q} \left[\sum_i \frac{p_i^2}{m} + \sum_i \frac{P_i^2}{M} + \sum_i \frac{p_{0i}^2}{m_0} - 4Nk_B T \right], \quad (11)$$

$$\frac{dV}{dt} = s \frac{\Pi}{M_{\Pi}}, \quad (12)$$

$$\frac{d\Pi}{dt} = \frac{s}{n_d V} \left[\sum_i \frac{p_i^2}{m} - \sum_i \left(\frac{\partial V^{\text{intra}}}{\partial r_i} + \frac{\partial V^{\text{inter}}}{\partial r_i} \right) r_i + \sum_i \frac{P_i^2}{M} - \sum_i \frac{\partial V^{\text{inter}}}{\partial X_i} \cdot X_i - n_d V P \right], \quad (13)$$

where V^{inter} stands for the summation of the intermolecular potentials for the nearest and next-nearest pairs, V^{ph} is the potential of Eq. (2), $n_d(=2)$ is the system dimension, and $\xi \equiv \frac{P_s}{Q}$.

Here, we assume that the totally symmetric vibration and intermolecular interactions determine the volume under a given pressure, but that the oscillator [Eq. (2)] does not have direct influence on the volume and only produces the entropy difference. It should be noted that Eq. (13), which gives the Virial theorem at equilibrium, does not contain the motion of the oscillator [Eq. (2)]. (Note that u_{0i} and p_{0i} are not rescaled by the system volume.) The details of the present formulation will be reported elsewhere.³⁰

We treat a system of $N=L^2=20 \times 20$ molecules with a periodic boundary condition, and employ an operator decomposition method in which the numerical error is $O(\Delta t^3)$.³¹ We set $m=1.0$, $M=1.0$, $m_0=1.0$, $M_{\text{II}}=0.2$, and $Q=1.0$.²¹ MD simulations were performed on a simple square lattice (V is the area or unit volume along the c axis), but the extension to three dimensions is straightforward.

First, we study the dependences of V and f_{HS} on T as functions of D . We define the normalized volume: $V_n = \frac{V-V_{\text{LS}}}{V_{\text{HS}}-V_{\text{LS}}}$, where V_{LS} (V_{HS}) is the volume for r_{LS} (r_{HS}). The HS fraction²⁴ is defined as $f_{\text{HS}} \equiv \langle \frac{1}{N} \sum_{i=1}^N \beta(x_i)^2 \rangle$, where $\langle \dots \rangle$ means the statistical average. Here, the system was warmed up from $T=0.1$ to 5.0 in steps of increment 0.1 under the pressure $P=0.001$, and then cooled down to the initial temperature $T=0.1$. At each temperature, 200 000 MD steps were discarded as transient time and the subsequent 100 000 MD steps were used to measure physical quantities with the MD time step $\Delta t=0.01$.

In Fig. 2, the dependences of f_{HS} and V_n on T are depicted for several values of D .³² The temperature dependence changes from a gradual crossover for small D [Fig. 2(a)] to a first-order transition for large D [Figs. 2(b)–2(d)]. In the warming process, f_{HS} increases and approaches a saturated value (<1), while V_n increases at high temperatures and finally exceeds 1. It is worth noting that V_n (V) has a linear dependence on T at high temperatures. This linear dependence has often been assumed in analyses of V - T curves in experiments with the use of phenomenological lattice expansion models.^{33,34} Here, we demonstrated this linear dependence which verifies this assumption from the viewpoint of a microscopic treatment. We estimate the thermal expansion $dV_n/dT=0.050$ at high temperatures ($2 \leq T \leq 5$) for (a) and $dV_n/dT=0.037$ for (b), indicating that the thermal expansion in the weaker interaction case is larger.

We find characteristic features for the T dependence of f_{HS} , which drastically change depending on D . In cases (a) and (b), f_{HS} continues to decrease in the cooling process. For larger D , i.e., cases (c) and (d), however, f_{HS} increases during the cooling process when the state is in the HS phase al-

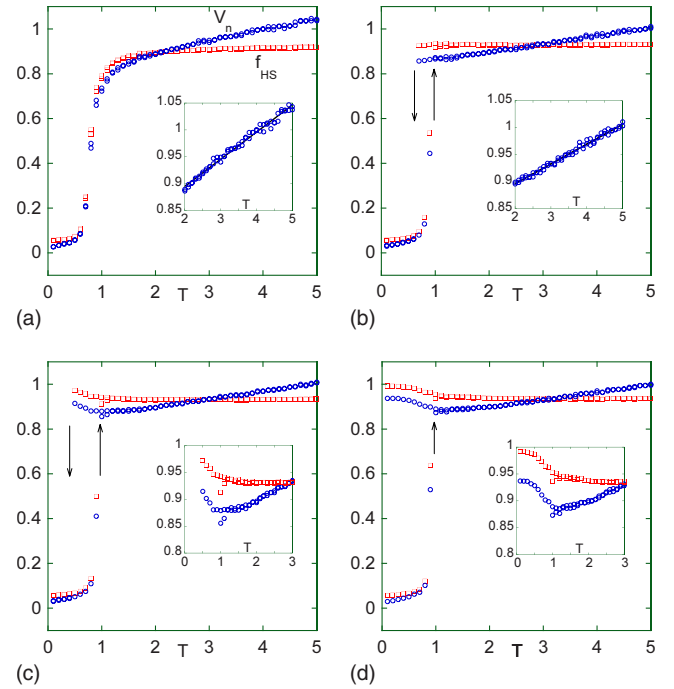


FIG. 2. (Color online) Temperature dependences of V_n (blue circles) and f_{HS} (red squares) for the values of (a) $D=5$, (b) $D=12$, (c) $D=12.9$, and (d) $D=15$ under $P=0.001$. Linear dependence of V_n is shown in the insets for (a) and (b). The T dependence around the region of the minimum V_n is focused on in the insets for (c) and (d).

though f_{HS} is almost constant at high temperatures. In these cases, the HS metastable state at low temperatures has larger f_{HS} at lower T . This is similar to the strong-interaction case of the short-range Ising-like model.¹²

We also find interesting observations of the T dependence of V_n , which exhibits different features from f_{HS} . For smaller D [(a) and (b)], V_n also decreases in the cooling process. For larger D , e.g., (c) and (d), in contrast to f_{HS} , V_n decreases during the cooling process at high temperatures, goes through a minimum value, and then increases again at lower T .

This suggests that at low temperatures where the metastable HS state exists, due to the small thermal fluctuation the state of the molecules tends to be around the minimum point of the HS intramolecular potential ($x=1$). At higher temperatures, the state of the molecules can change over the barrier to the LS state and some HS molecules change to LS molecules. Consequently, the volume is reduced. Therefore, the derivative of V , $\frac{\partial V}{\partial T}$, is negative, which leads to negative thermal expansion.

Next, we focus on the relaxation dynamics from the excited HS state. We observe the relaxation from the HS metastable state.^{3,12} Figure 3 shows relaxation curves for various T and P . It is found that relaxations occur with sigmoidal curves at various T . In the case of $T=0.15$, the relaxation does not occur within the measurement time, and when the temperature is increased, the relaxation speed is accelerated.

If higher pressure P is applied [Fig. 3(b)] because the LS state is favored, the decay time becomes shorter. The meta-

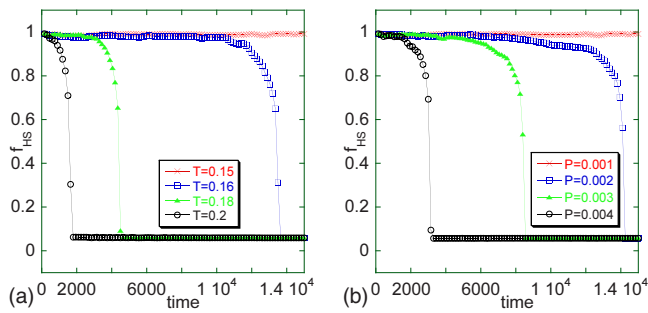


FIG. 3. (Color online) (a) T dependence of the relaxation curve of f_{HS} from the HS state at $P=0.001$ for $D=12$. (b) P dependence of the relaxation curve of f_{HS} from the HS state at $T=0.15$ for $D=12$.

stable state becomes unstable, not only with temperature but also with pressure. It should be noted that the sigmoidal shape is maintained at different P , which is consistent with experiments.²⁶ We have shown that f_{HS} relaxes with a sigmoidal curve. This dependence is attributed to the self-acceleration mechanism due to the local energy barrier and

cooperativity. Here, sigmoidal relaxations are automatically yielded as a result of the deterministic dynamics.

We have studied the characteristics of T and P dependences of f_{HS} and V developing a model of elastic interactions and a method of MD. A nonmonotonic temperature dependence of V has been demonstrated. Negative and zero thermal expansions³⁵ are one of the topics of molecular solids. Our observation will promote researches for the unusual behavior of thermal expansion. Typical sigmoidal relaxations with T and P dependences from the excited high-spin state (photoinduced state) are automatically reproduced as a result of the deterministic MD dynamics. To our knowledge, this is the first observation of sigmoidal curves from deterministic dynamics based on a microscopic model of SC.

The authors would like to thank H. Tokoro for useful discussion and also thank P. A. Rikvold for critical reading. The present work was supported by Grant-in-Aid for Scientific Research from MEXT of Japan. The numerical calculations were supported by the supercomputer center of ISSP of Tokyo University.

*Corresponding author; nishino.masamichi@nims.go.jp

- ¹S. Decurtins, P. Gütllich, C. P. Köhler, H. Spiering, and A. Hauser, *Chem. Phys. Lett.* **105**, 1 (1984).
- ²J. A. Real, H. Bolvin, A. Bousseksou, A. Dworkin, O. Kahn, F. Varret, and J. Zarembowitch, *J. Am. Chem. Soc.* **114**, 4650 (1992).
- ³P. Gütllich, A. Hauser, and H. Spiering, *Angew. Chem. Int. Ed. Engl.* **33**, 2024 (1994) and references therein.
- ⁴O. Kahn and C. Jay Martinez, *Science* **279**, 44 (1998).
- ⁵J. F. Létard, J. A. Real, N. Moliner, A. B. Gaspar, L. Capes, O. Cador, and O. Kahn, *J. Am. Chem. Soc.* **121**, 10630 (1999).
- ⁶A. Hauser, J. Jeftić, H. Romstedt, R. Hinek, and H. Spiering, *Coord. Chem. Rev.* **190-192**, 471 (1999).
- ⁷M. Sorai, *Bull. Chem. Soc. Jpn.* **74**, 2223 (2001).
- ⁸J. Wajnlasz and R. Pick, *J. Phys. (Paris), Colloq.* **32**, C1-91 (1971).
- ⁹A. Bousseksou, J. Constant-Machado, and F. Varret, *J. Phys. I* **5**, 747 (1995).
- ¹⁰K. Boukheddaden, I. Shteto, B. Hôo, and F. Varret., *Phys. Rev. B* **62**, 14796 (2000); **62**, 14806 (2000).
- ¹¹M. Nishino, S. Miyashita, and K. Boukheddaden, *J. Chem. Phys.* **118**, 4594 (2003).
- ¹²S. Miyashita, Y. Konishi, H. Tokoro, M. Nishino, K. Boukheddaden, and F. Varret, *Prog. Theor. Phys.* **114**, 719 (2005).
- ¹³R. Zimmermann and E. König, *J. Phys. Chem. Solids* **38**, 779 (1977).
- ¹⁴T. Kambara, *J. Phys. Soc. Jpn.* **50**, 2257 (1981).
- ¹⁵P. Adler, L. Wiehl, E. Meißner, C. P. Köhler, H. Spiering, and P. Gütllich, *J. Phys. Chem. Solids* **48**, 517 (1987).
- ¹⁶N. Willenbacher and H. Spiering, *J. Phys. C* **21**, 1423 (1988).
- ¹⁷A. L. Tchougréeff and M. B. Darkhovskii, *Int. J. Quantum Chem.* **57**, 903 (1996).
- ¹⁸H. Spiering, *Top. Curr. Chem.* **235**, 171 (2004).
- ¹⁹J. A. Nasser, K. Boukheddaden, and J. Linares, *Eur. Phys. J. B* **39**, 219 (2004).
- ²⁰K. Boukheddaden, *Prog. Theor. Phys.* **112**, 205 (2004).
- ²¹M. Nishino, K. Boukheddaden, Y. Konishi, and S. Miyashita, *Phys. Rev. Lett.* **98**, 247203 (2007).
- ²²S. Miyashita, Y. Konishi, M. Nishino, H. Tokoro, and P. A. Rikvold, *Phys. Rev. B* **77**, 014105 (2008).
- ²³Y. Konishi, H. Tokoro, M. Nishino, and S. Miyashita, *Phys. Rev. Lett.* **100**, 067206 (2008).
- ²⁴K. Boukheddaden, M. Nishino, and S. Miyashita, *Phys. Rev. Lett.* **100**, 177206 (2008).
- ²⁵J.-P. Tuchagues, A. Bousseksou, G. Molnár, J. J. McGarvey, and F. Varret, *Top. Curr. Chem.* **235**, 85 (2004) and references therein.
- ²⁶J. Jeftić and A. Hauser, *J. Phys. Chem.* **101**, 10262 (1997).
- ²⁷S. Nosé, *J. Chem. Phys.* **81**, 511 (1984).
- ²⁸W. G. Hoover, *Phys. Rev. A* **31**, 1695 (1985).
- ²⁹H. C. Andersen, *J. Chem. Phys.* **72**, 2384 (1980).
- ³⁰M. Nishino, *et al.* (unpublished).
- ³¹M. Suzuki, *Phys. Lett. A* **146**, 319 (1990).
- ³²The unit of the temperature, i.e., the unit of the energy, should be chosen to reproduce experiments, e.g., 100 K.
- ³³E. Meissner, H. Köppen, H. Spiering, and P. Gütllich, *Chem. Phys. Lett.* **95**, 163 (1983).
- ³⁴L. Wiehl, G. Kiel, C. P. Köller, H. Spiering, and P. Gütllich, *Inorg. Chem.* **25**, 1565 (1986).
- ³⁵T. Matsuda, H. Tokoro, K. Hashimoto, and S. Ohkoshi, *Dalton Trans.* **42**, 5046 (2006).